Platforms for 1D topological superconductivity

Ady Stern (Weizmann)

Outline

1. Short advertisement
2. The rest of the talk

Outline

1. Short advertisement

2. The rest of the talk:

   a. One dimensional topological superconductors-background
   b. Phase controlled 1D topological superconductivity
   c. Disorder

1. The Quantum Hall effect
2. Topological superconductivity
3. Topological universe on a graphene sheet
4. Topological insulators
5. Topological classification
6. Gapless topological phases
7. Material prediction
8. States of topological Order
9. Experimental tools

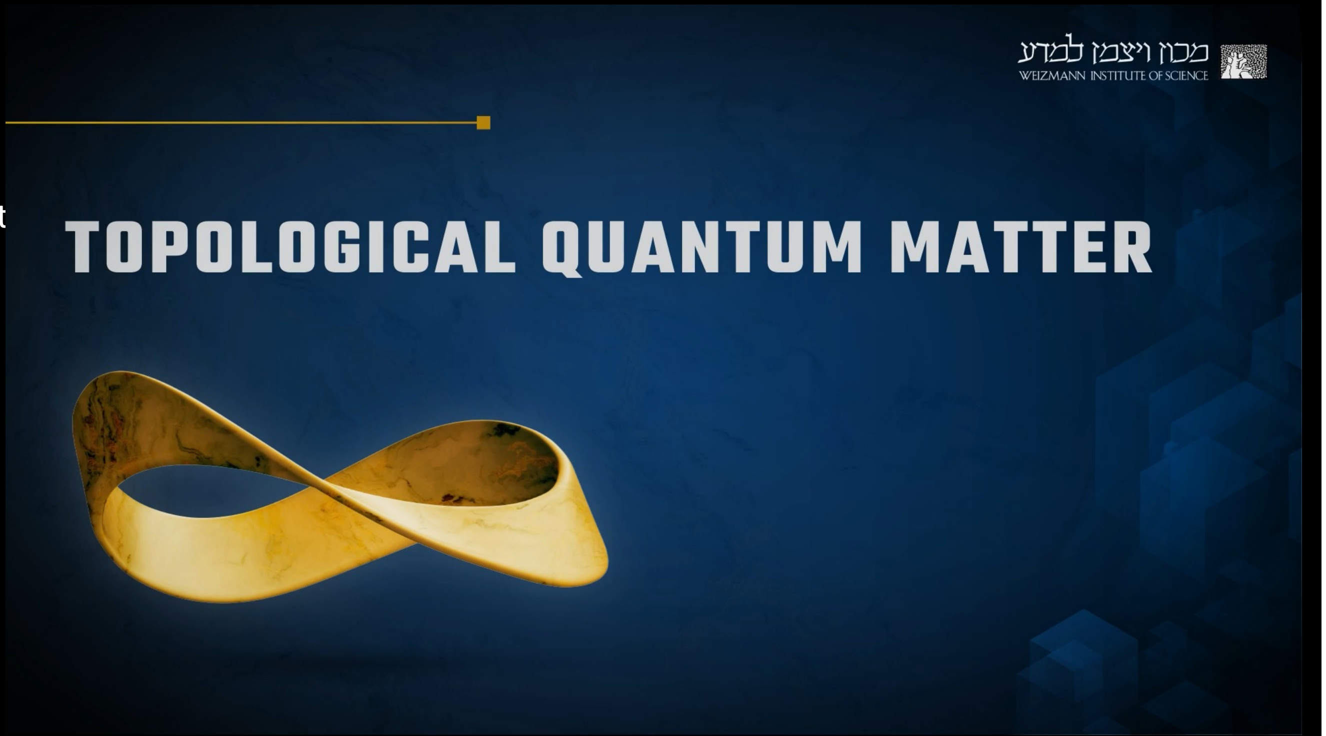

On EDX, CampusIL & Youtube

Search for *Topological quantum matter Weizmann online*

1D topological superconductivity – background

One dimensional superconductors are

1. Exciting – localized Majorana zero modes, topological protection, non-abelian statistics, topological quantum information processing

2. Based on a straightforward theory

3. Are harder to realize, control and explore than they could have been

Perhaps we have not yet found the best experimental set-up…

1D topological superconductors and Majorana zero energy modes

(Kitaev, Read&Green, Kopnin, Saloma)

BdG Hamiltonian

$$H = H_0 + \int dr \Delta(r) \Psi^+ \partial \Psi^+ + h.c.$$

A quadratic Hamiltonian!

1D topological superconductors and Majorana zero energy modes

(Kitaev, Read&Green, Kopnin, Saloma)

BdG Hamiltonian

$$H = \begin{pmatrix}\psi^+ & \psi\end{pmatrix}\begin{pmatrix}H_0 & \Delta \\ \Delta^+ & -H_0\end{pmatrix}\begin{pmatrix}\psi \\ \psi^+\end{pmatrix}$$

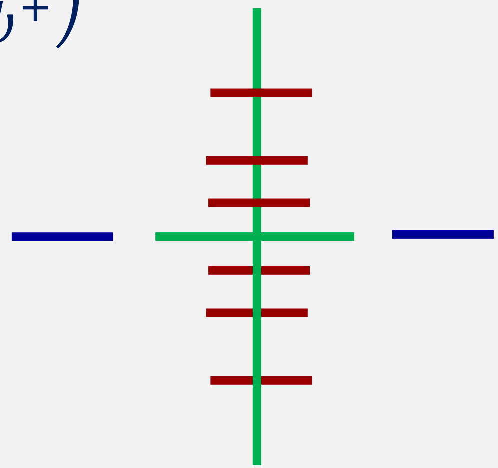

a matrix with two important properties:

- Even dimensional
- Spectrum is symmetric around zero energy

⇒ An even number of zero energy states

⇒ Two well separated zero energy modes are protected

- A topologically protected degeneracy of the ground state
- Opens up possibilities for topologically protected unitary evolution, topological qubits etc.

Topological Superconductivity in Nanowires

Quantum wire with spin-orbit coupling and Zeeman field:

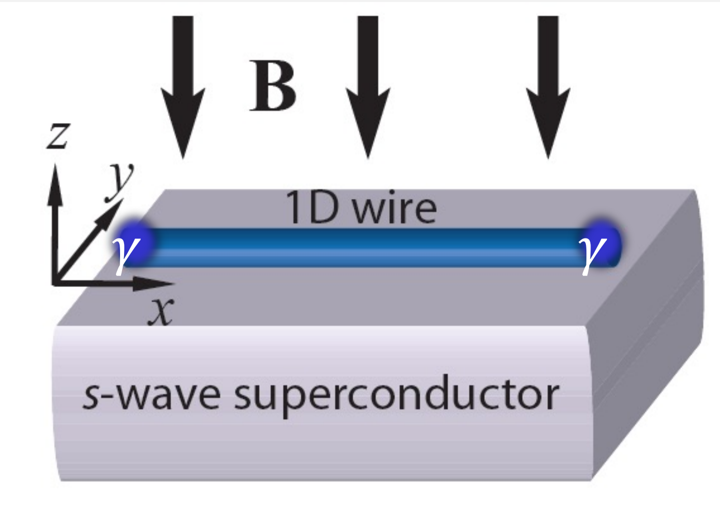

$$H_0 = \frac{k_x^2}{2m} - \mu + \alpha k_x \sigma_y + B\sigma_z$$

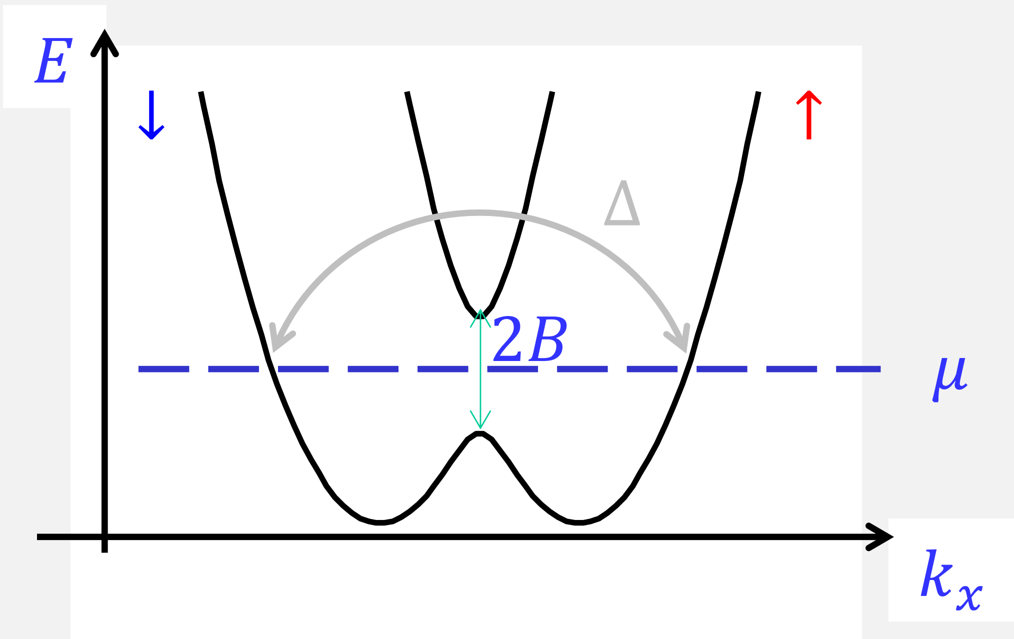

Lutchyn et al. PRL 2010
Oreg et al. PRL 2010

Requires fine-tuning of μ!

figure taken from
Alicea, Rep. Prog. Phys. (2012)

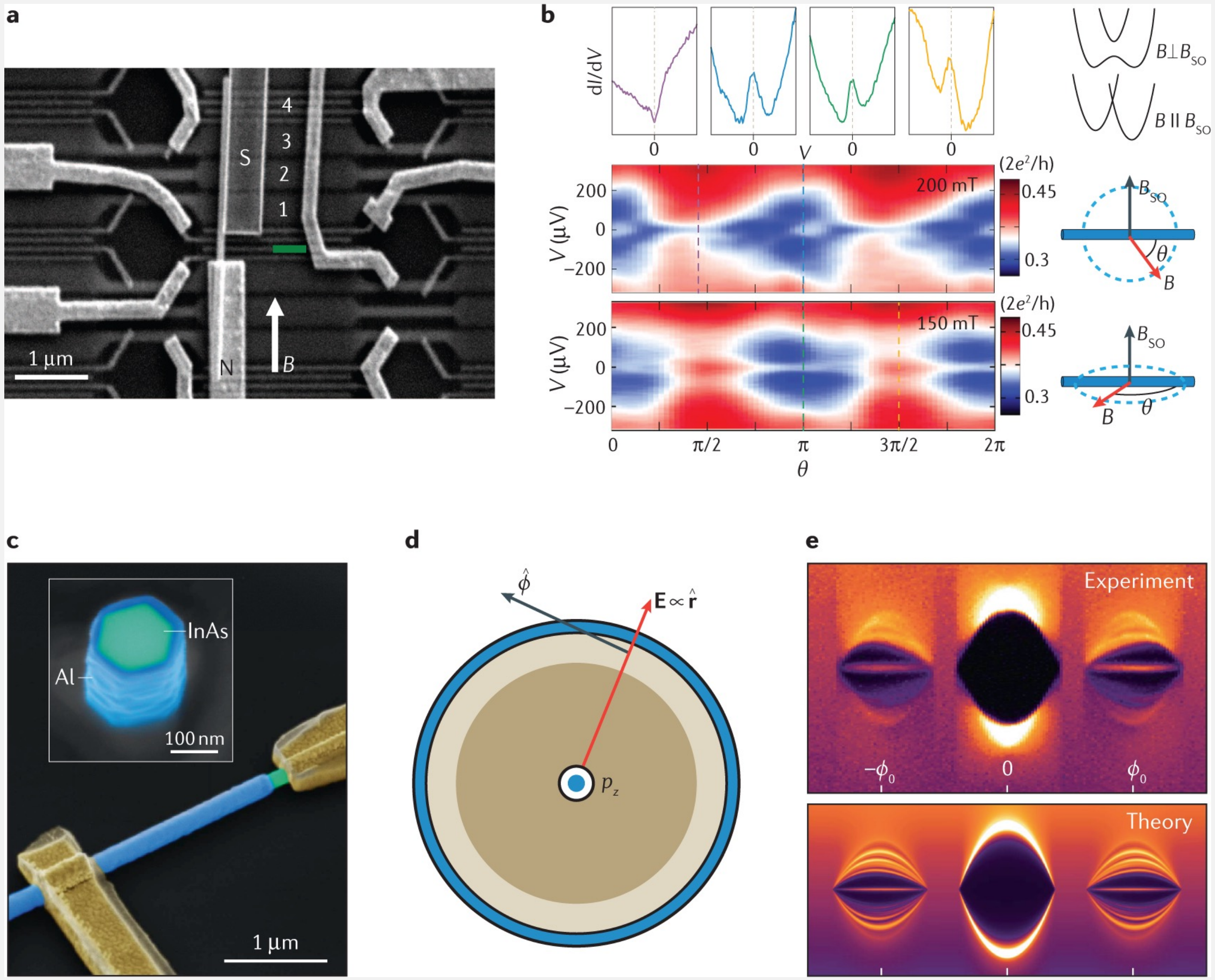

Mourik, V. et al. *Science* **336**, 1003–1007 (2012)
Vaitiekenas, S. et al. *Science* **367**, eaav3392 (2020)

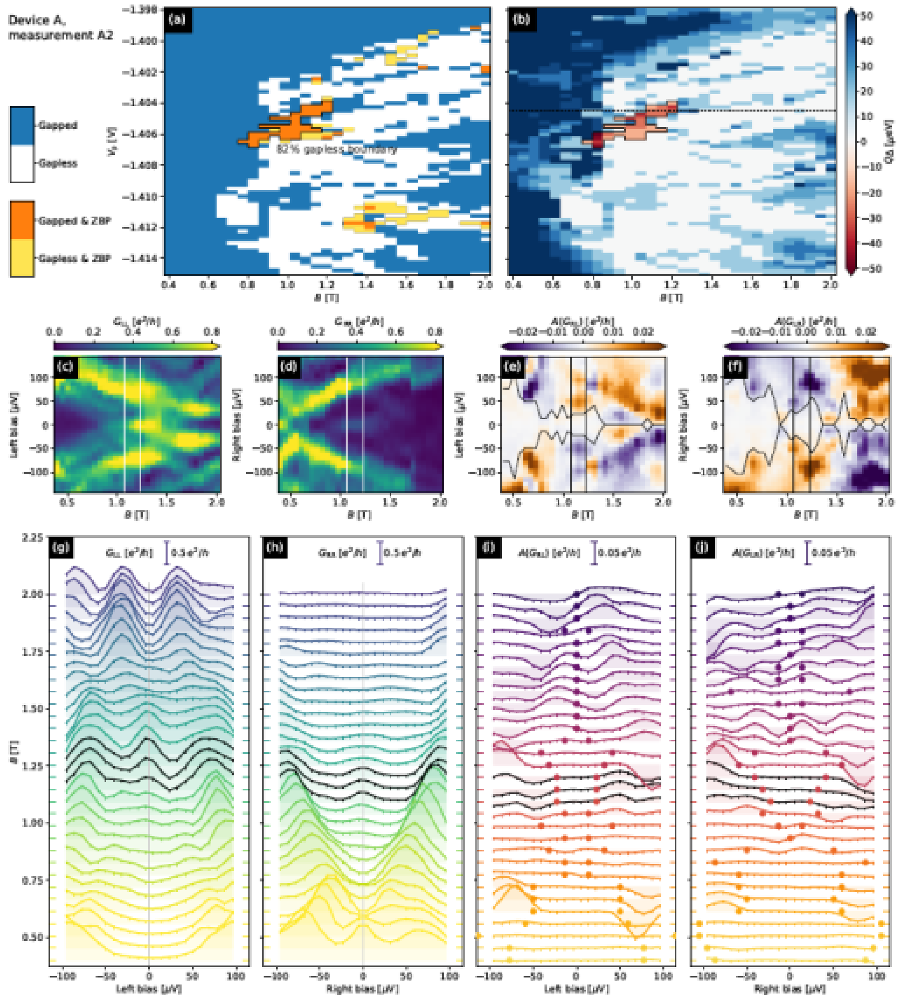

FIG. 11. (a) The experimental phase diagram of device A (measurement A2) that results from combining the clusters of stable ZBPs at both junctions with the map of the locus of zero/non-zero gap. The stability of ZBPs is determined by varying the cutter gate settings so that both $B = 0$ conductances take the values $0.3, 0.5, 0.7, 0.9e^2/h$ at an above-gap bias voltage of $500\,\mu$V. The boundary of the ROI_2 is interpreted as a phase transition line, consistent with a visible gap closure along 82% of it. (b) The experimental phase diagram, showing trivial/topological phases, which the TGP identifies with the exterior/interior ($Q = \pm 1$) of the ROI_2. The color scale shows the size of the trivial (positive sign) or topological (negative sign) gap. The protocol assigns a maximum topological gap $\Delta_{\mathrm{topo}}^{\mathrm{max}} = 29\,\mu$eV. Measured local and antisymmetrized non-local conductances along the horizontal line in panel b at $V_{\mathrm{p}} = -1.4045$ V: (c) G_{LL}, (d) G_{RR}, (e) $A(G_{\mathrm{RL}})$, (f) $A(G_{\mathrm{LR}})$. The ROI_2 lies between the vertical lines. Panels (g)-(j) are "waterfall" plots representing the same measured data. The data shown in (c)-(j) was obtained for above-gap left (right) conductances of approximately $0.5e^2/h$ ($0.8e^2/h$). The black curves in panels (e) and (f) and the dots in panels (i) and (j) indicate where the non-local signal drops below a threshold value, as described in the text.

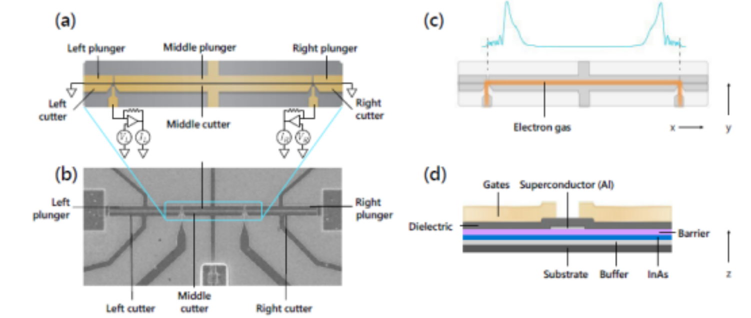

(Aghaee et al., 2022)

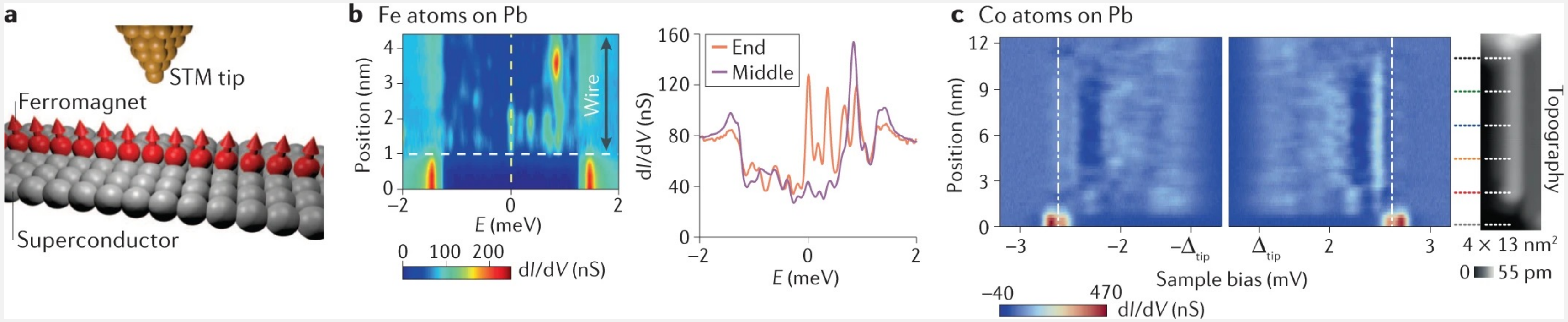

Nadj-Perge, S. et al. *Science* **346**, 602–607 (2014)
Feldman, B. E. et al. *Nat. Phys.* **13**, 286–291 (2017)
Ruby, M., et al., *Nano Lett.* **17**, 4473–4477 (2017).

Difficulties:

- Uneasy coexistence of superconductivity and magnetic field
- Uneasy coexistence of gating and superconductivity
- Disorder

One dimensional superconductors are

1. Exciting – localized Majorana zero modes, topological protection, non-abelian statistics, topological quantum information processing

2. Based on a straightforward theory

3. Are harder to realize, control and explore than they could have been

Perhaps we have not yet found the best experimental set-up…

Introducing another knob – the superconducting phase

1. Introduce a 1D superconducting system

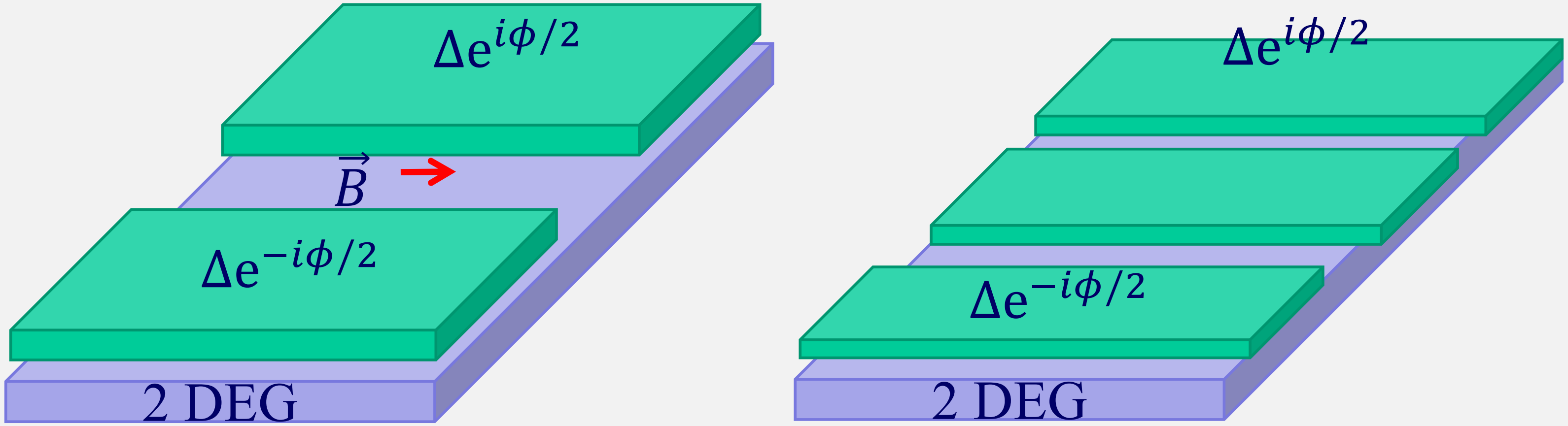

2. Impose periodic boundary conditions ⇒ k_x is well defined. Solve the BdG spectrum as a function of k_x.

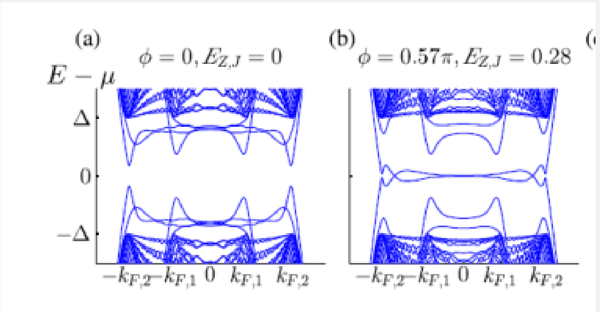

3. Search for single gap-closing points at $k_x = 0$. These are trivial ⟺ topological transition points (Kitaev)

- Focus at $k_x = 0$ (Kitaev)
- Solve BdG equation

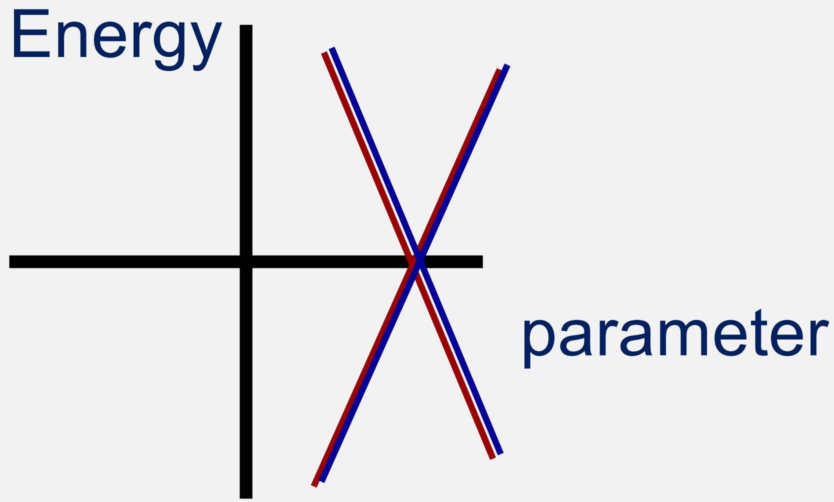

Spin symmetry must be broken!

1D topological superconductor in a 2D setting

(Pientka, Keselman, Yacoby, Berg, Stern, Halperin) (Hell et al.)

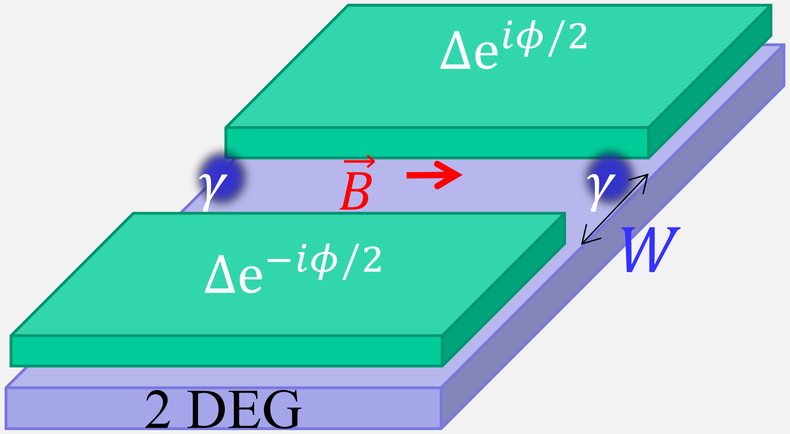

Ingredients:
- ✓ 1D
- ✓ Spin-orbit
- ✓ Superconductivity
- ✓ Magnetic field

New knobs to tune – phase difference, Josephson current, enclosed magnetic flux

New features:

- Robust topological phase with no fine-tuning (for $\phi \approx \pi$)
- Can tune itself the topological phase!

Robust topological phase with no fine-tuning (for $\phi \approx \pi$)

Phase difference

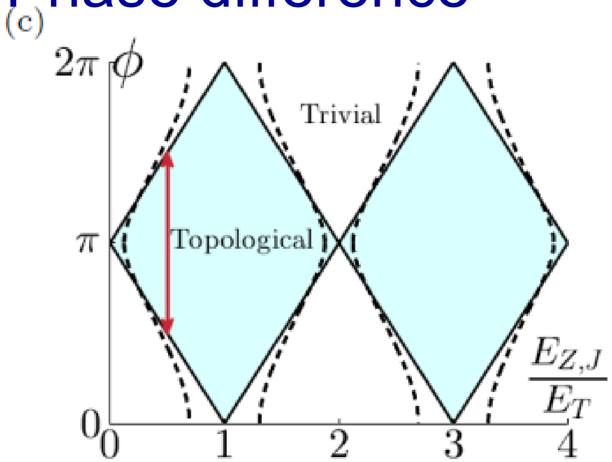

Zeeman energy * traversal time

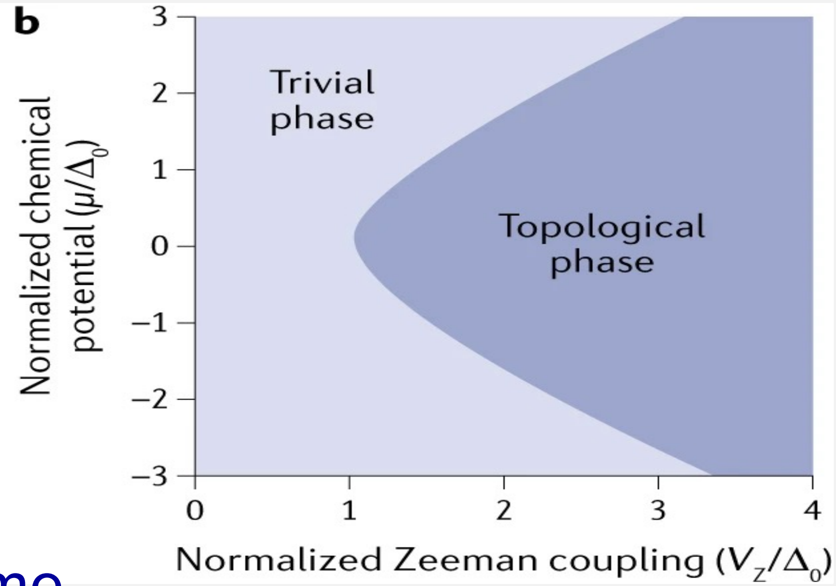

Only weak dependence on the chemical potential
(Spin orbit energy >> Zeeman energy, wide superconductors)

First order phase transition between trivial and topological state – the system self tunes to the topological regime

The phase difference at the ground state:

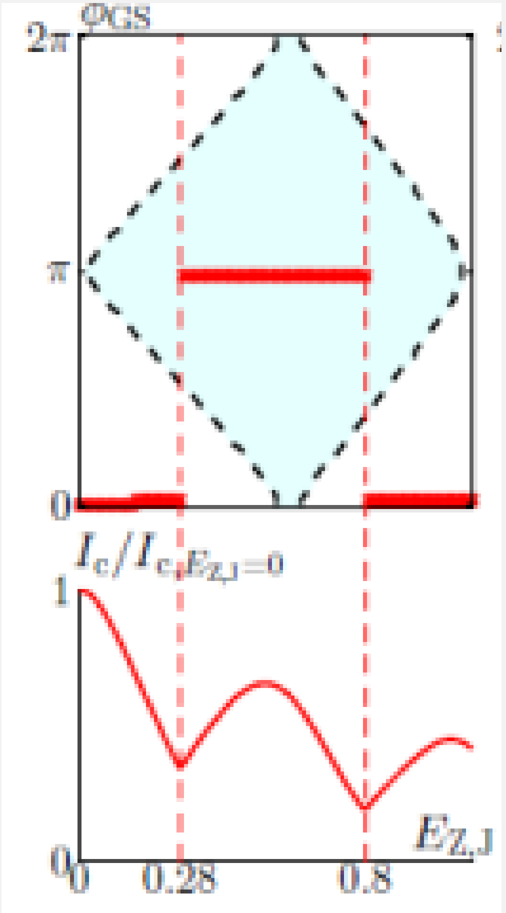

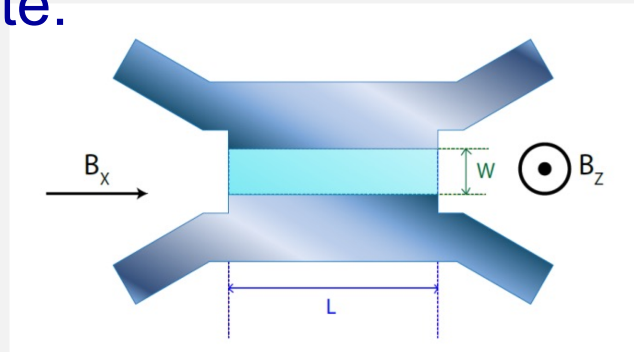

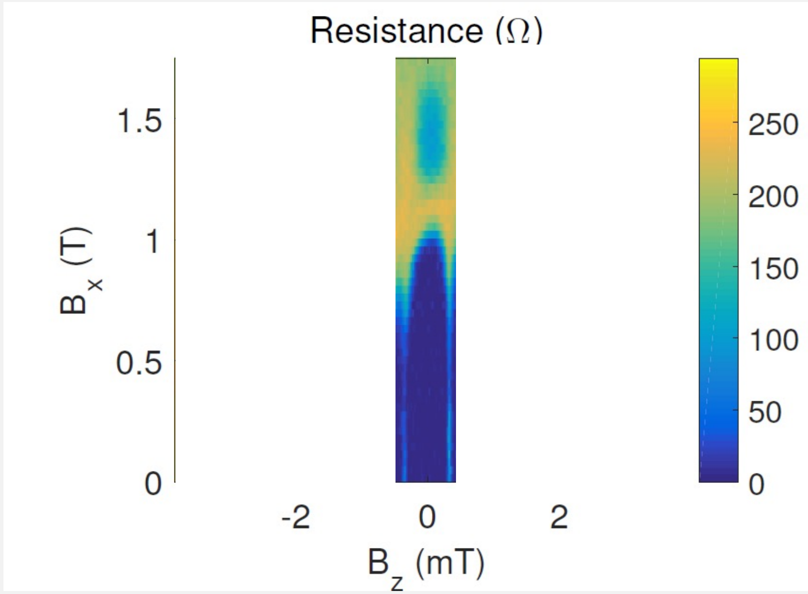

Hart et al. (2015)

The transition coincides with a minimum of the critical current.

Setup and Model

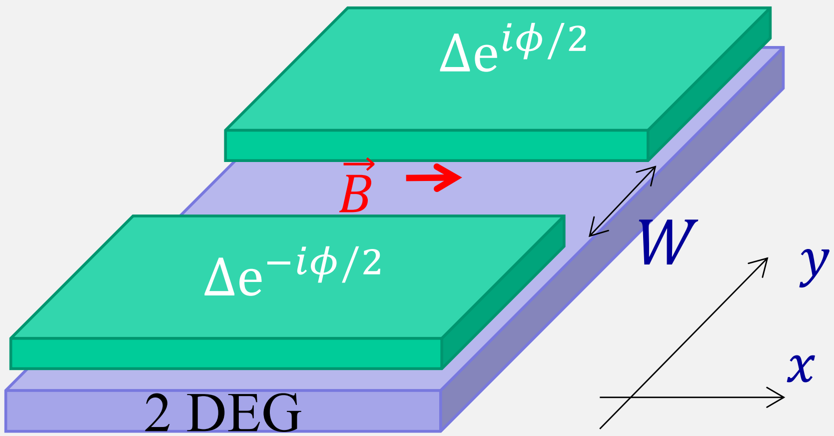

Hamiltonian in the normal region:

$$H_0 = \frac{k_x^2 + k_y^2}{2m} - \mu + \alpha\left(k_x\sigma_y - k_y\sigma_x\right) + B_x\sigma_x$$

$$H_0 = \frac{k_x^2 - \partial_y^2}{2m} - \mu + \alpha\left(k_x\sigma_y + i\partial_y\sigma_x\right) + B_x\sigma_x$$

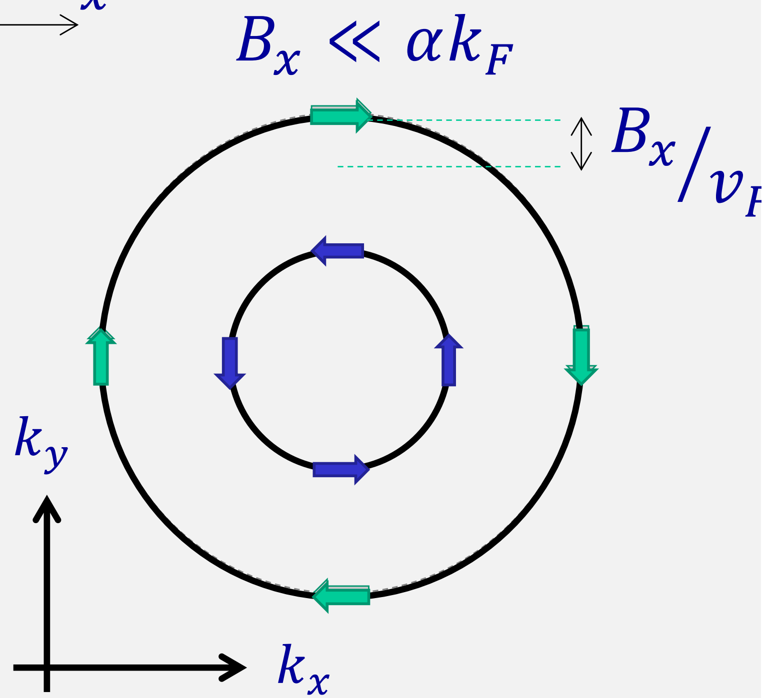

We are looking for states within the gap, bound between the two superconductors

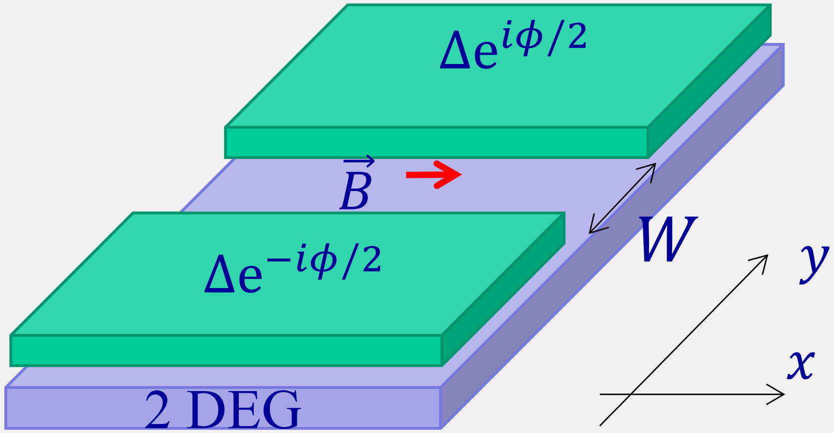

Almost the particle in the box problem, except the boundary conditions - Andreev processes

For distinguishing topological from trivial, we need to look at k_x=0

For the ground state energy and energy gap, we need all k_x

Andreev bound state spectrum, $\Delta \ll \mu$:

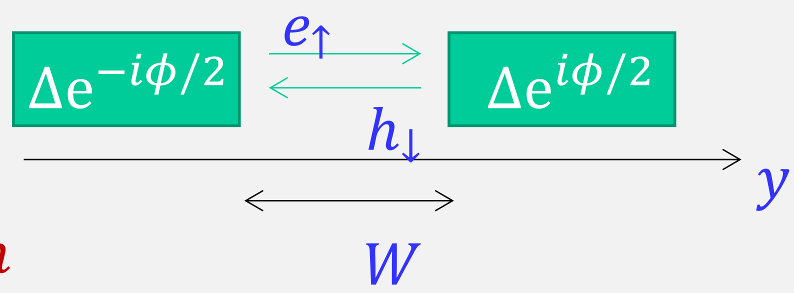

$$2\cos^{-1}\frac{E_n}{\Delta} + \phi + 2\frac{E_n}{v_F}W \pm 2\frac{B_x}{v_F}W = 2\pi n$$

phase acquired upon Andreev reflection

phase acquired upon traversing the junction

Narrow junction, i.e. $\Delta \ll {}^{v_F}/_{W}$: $E_n = \Delta\cos\left(\frac{\phi}{2} \pm \frac{B_x}{v_F}W\right) = \Delta\cos(\frac{\phi}{2} \pm \phi_B)$

Phase Diagram

k_x=0 bound states:

$$E_n = \Delta\cos\left(\frac{\phi}{2} \pm \frac{B_x}{v_F}W\right)$$

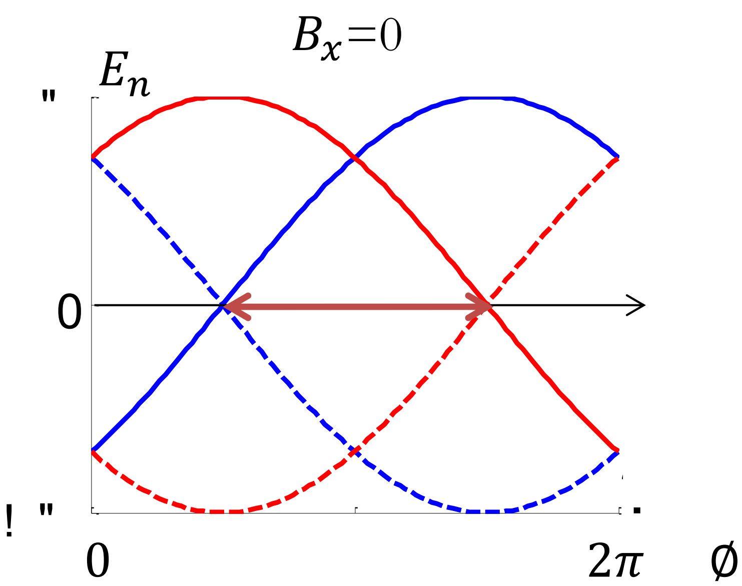

State is doubly degenerate!

Gap closing lines (for any W):

$$\phi \pm 2\frac{B_x}{v_F}W = (2n+1)\pi$$

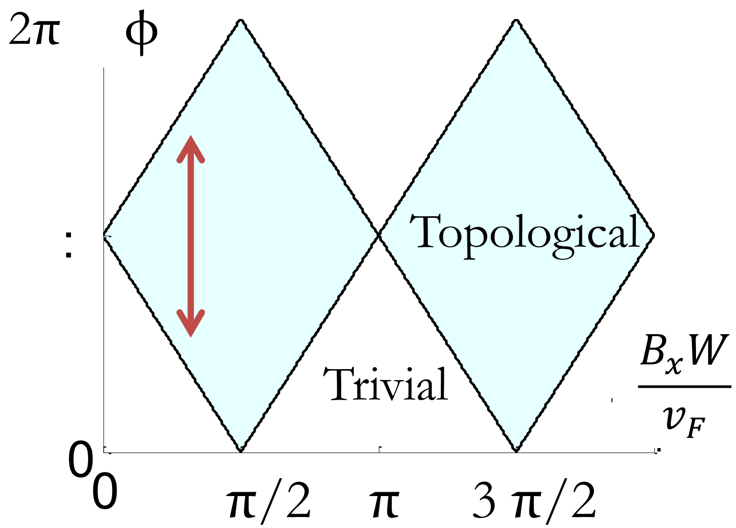

Insensitive to μ!

Majorana end states

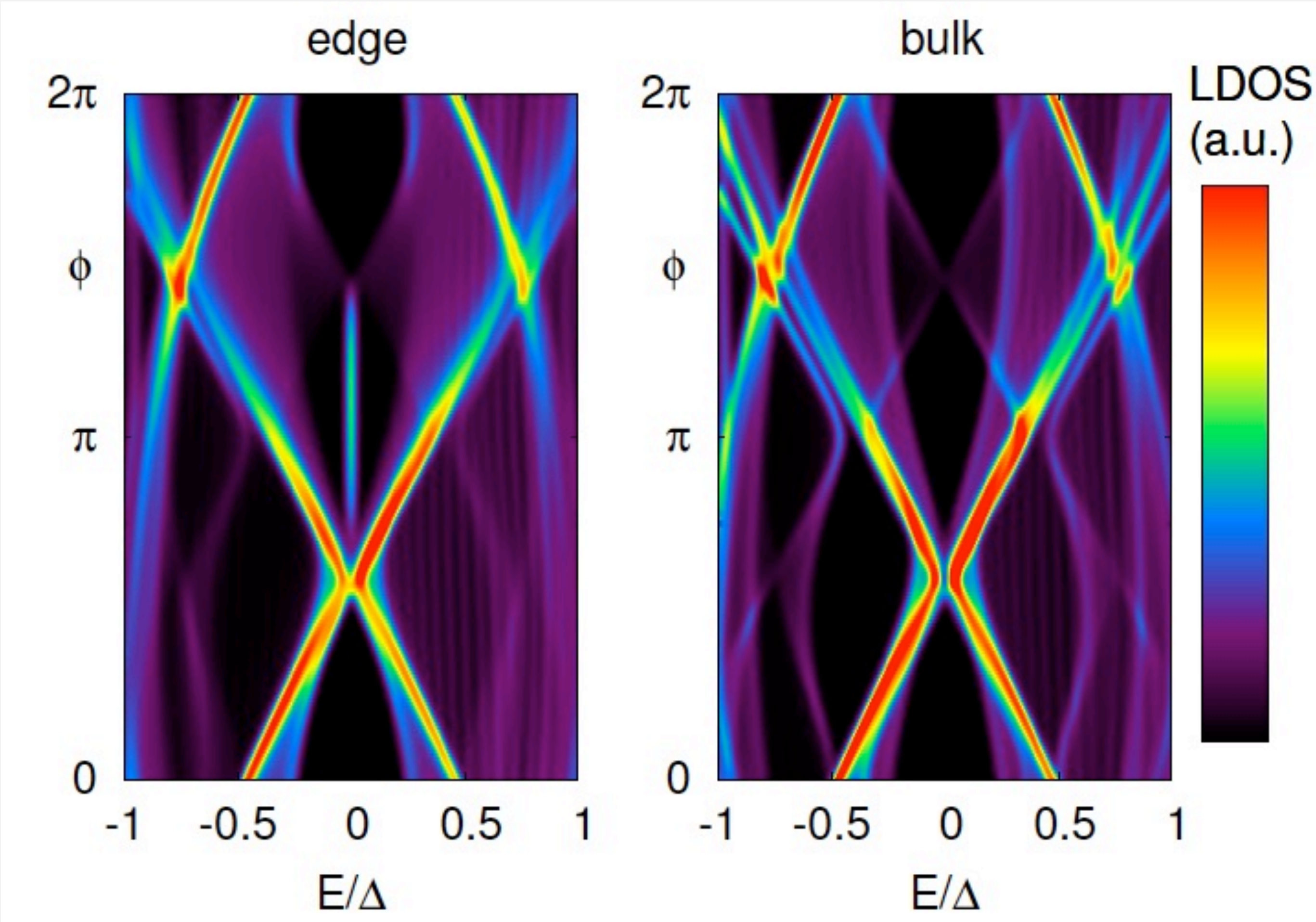

Experiments – Nichele - Marcus group (NBI)

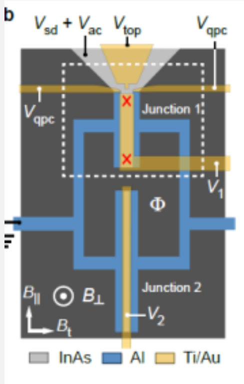

Measuring the tunneling density of states at the end of the junction

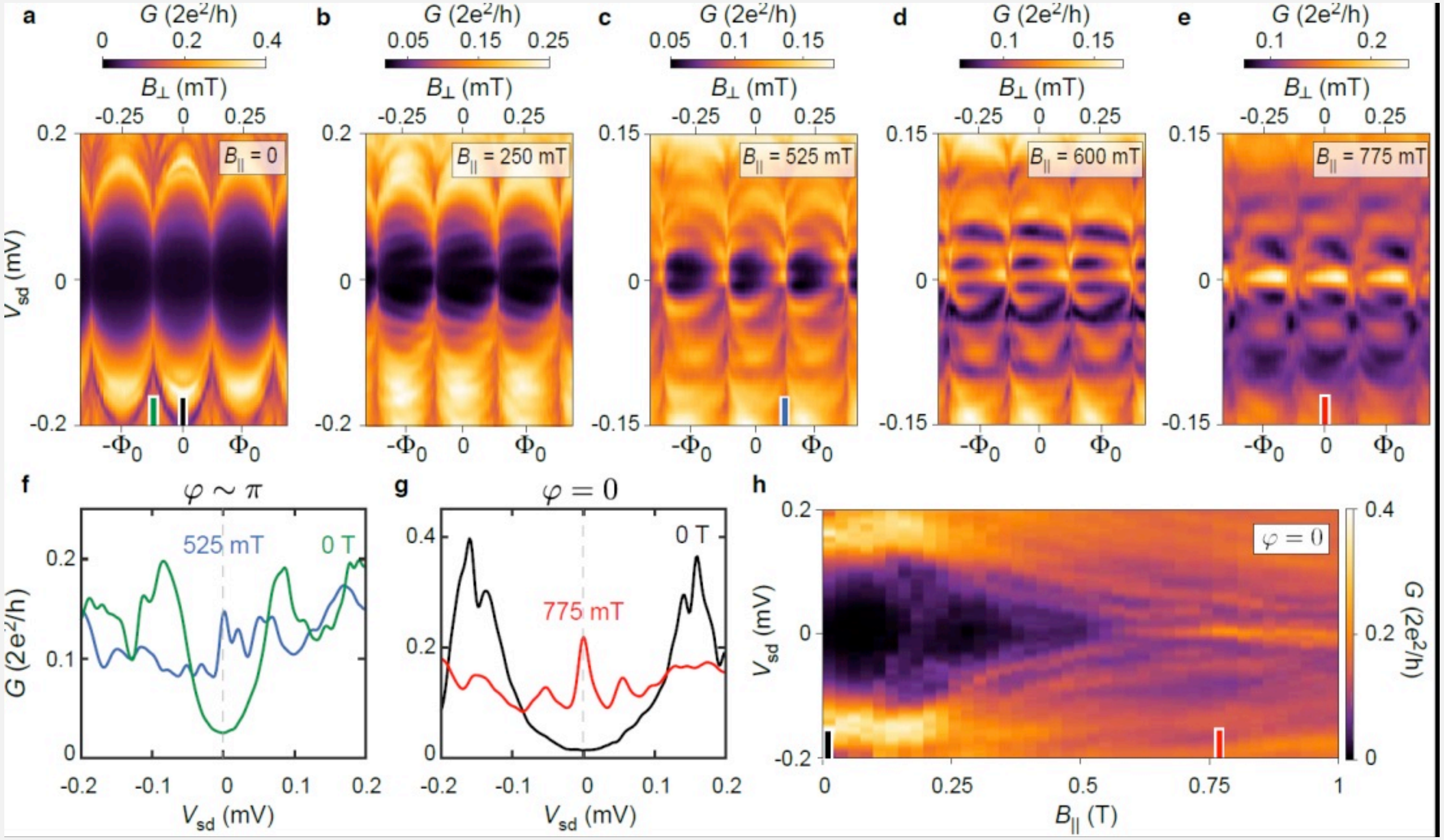

Improved set-up

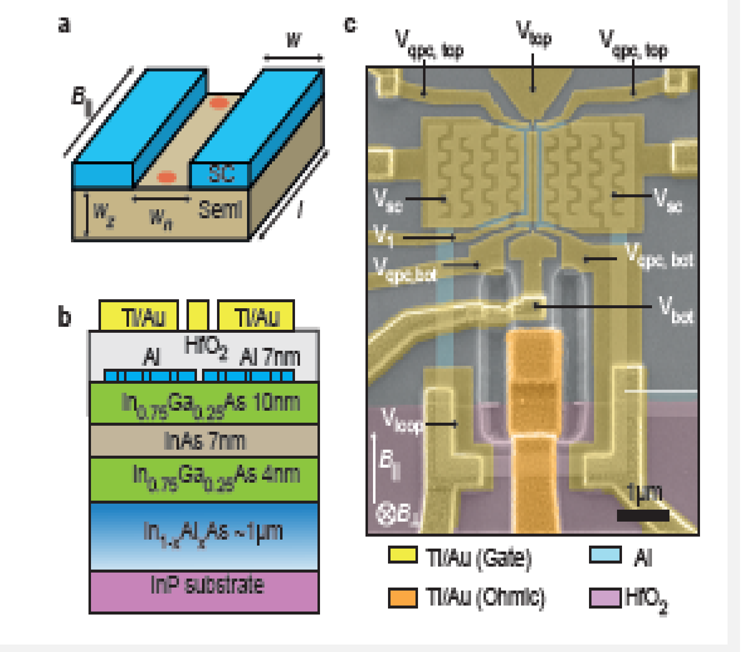

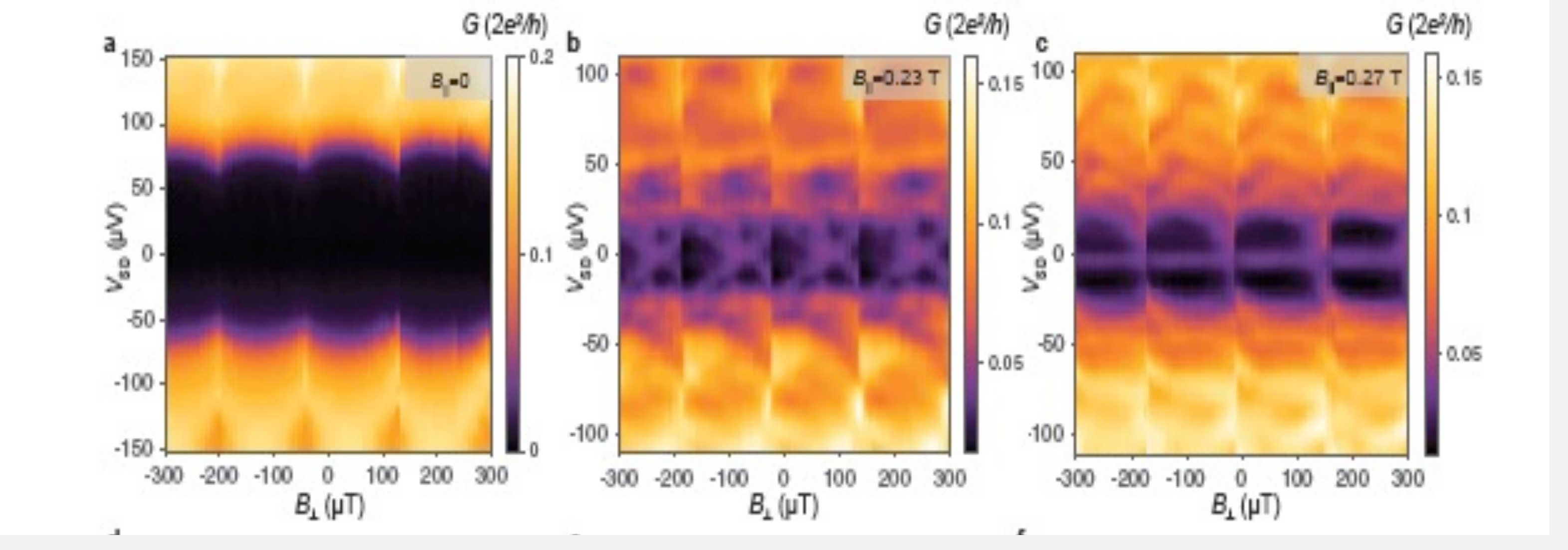

(Banerjee et al., 2022)

Experiments – Yacoby group (Harvard)

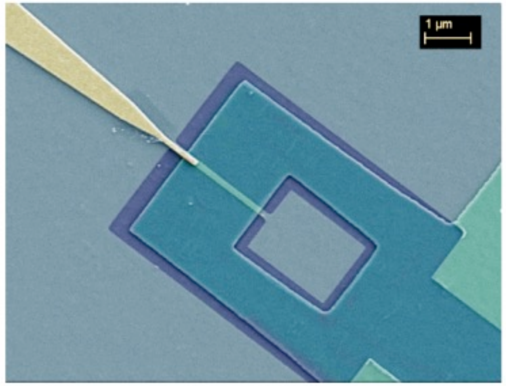

Measuring the tunneling density of states at the end of the junction

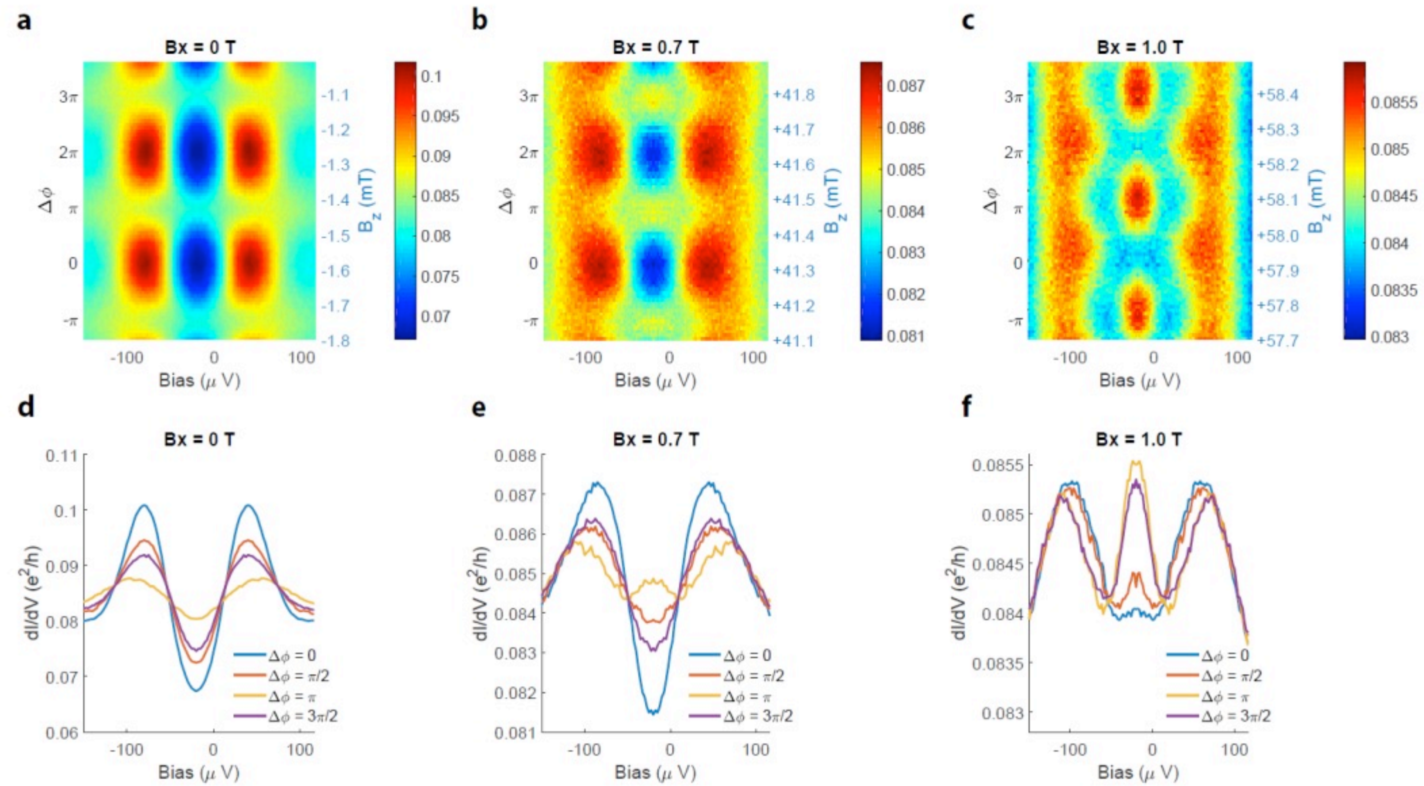

Experiments – Goswami group (Delft)

Measurement of the recovery of the critical current with increasing parallel magnetic field

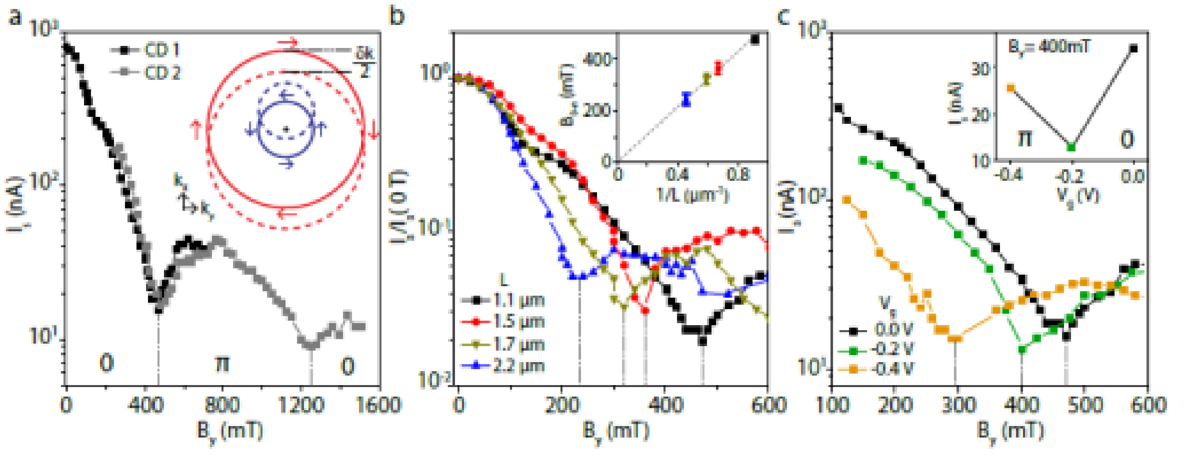

FIG. 2. | **Magnetic field-driven $0-\pi$ transitions.** **a,** Variation of the switching current, I_s, with in-plane magnetic field, B_y, at $V_g = 0$ V for the same JJ as in Fig. 1b,c. Two distinct revivals of I_s are visible at $B_y = 470$ mT and 1250 mT, associated with $0-\pi$ transitions. The data is from two cool downs (CDs). The momentum shift, $\delta k/2$, of the Fermi surfaces due to the Zeeman field is sketched in the inset. The solid (dashed) lines depict the situation at zero (finite) magnetic field, and the arrows represent the spin orientation. **b,** I_s as a function of B_y at $V_g = 0$ V for four JJs with different lengths. For better visibility, I_s is normalized with respect to I_s at $B_y = 0$ T. Dashed lines indicate $B_{0-\pi}$, the field at which the transition occurs for each length. The inset shows a linear dependence of $B_{0-\pi}$ on $1/L$, in agreement with ballistic transport. **c,** I_s vs. B_y at three different V_g for the JJ with $L = 1.1$ μm. $B_{0-\pi}$ shifts to lower values of B_y with more negative gate voltages. I_s vs. V_g at $B_y = 400$ mT shows a non-monotonic behavior as displayed in the inset. The length and gate dependence of panel **b** and **c** are in qualitative agreement with Eq. 1.

Eliminating the magnetic field altogether

(Lesser, Oreg, Stern, 2022)
(generalize earlier settings by
Lesser et al.+the NBI group, 2020-2022)

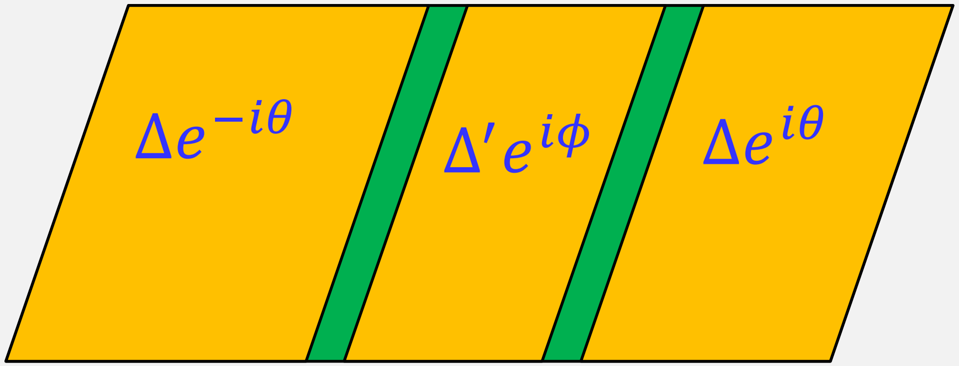

- SNSNS junction – two phase differences
- Different velocities of the two spin branches in the two superconductors

How do you recognize a 1D topological SC (theoretical level)

Focus on $k_x = 0$ (Kitaev)

- Single gap closing signifies a topological phase transition

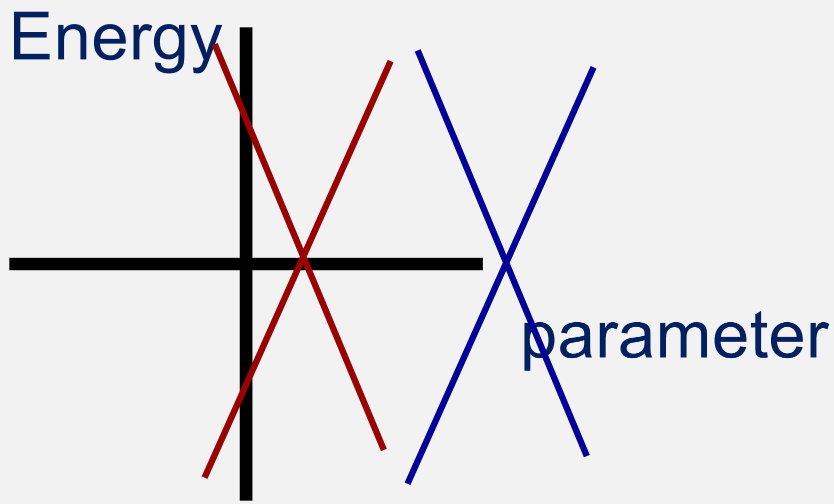

⇒ spin branches must be separated

One dimension – two spin branches in each direction.

Several ways to separate them:

- In real space –

Fu

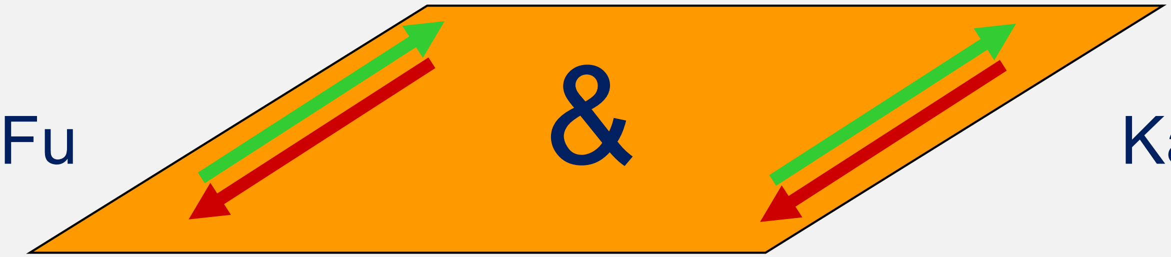

Kane

- In momentum space –

Oreg

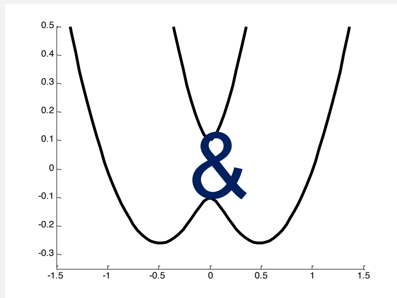

Lutchyn

- In energy –

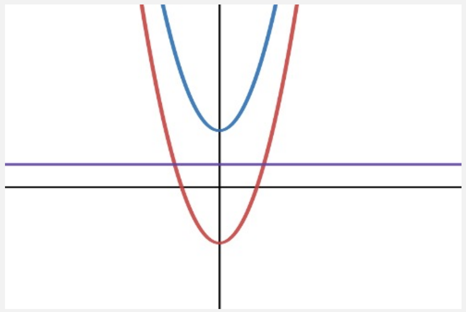

Kitaev

Now – in velocities

Start from -

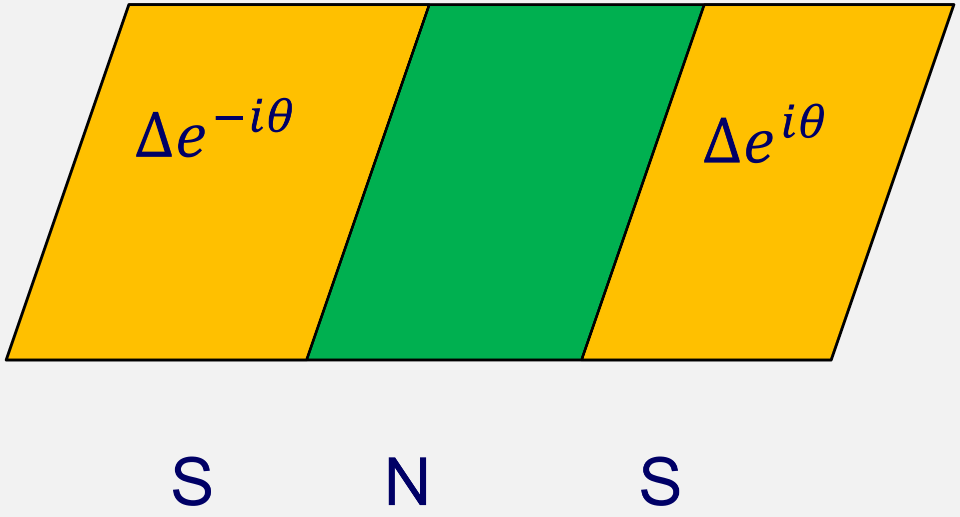

Two gap closings occur at $\theta = \pm\pi/2$.

May be separated by the application of a Zeeman parallel magnetic field. (Hell et al., Pientka et al.)

$$E_n = \Delta\cos\left(\frac{\phi}{2} \pm \frac{B_x}{v_F} W_N\right)$$

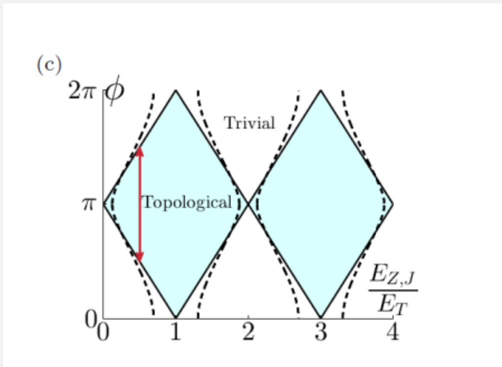

Experiments by Ren et al. Fornieri et al., Banergee et al.

Instead of the magnetic field -

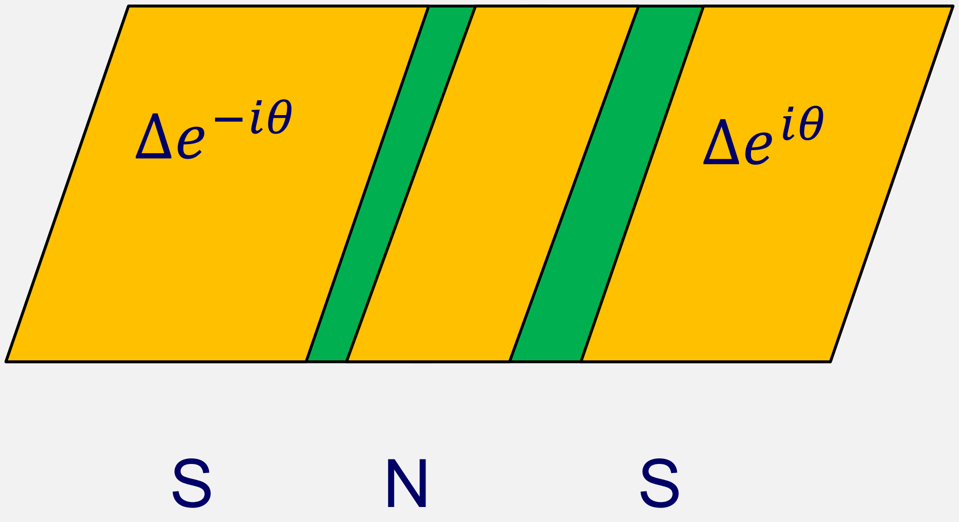

add a third superconductor in the middle with $\Delta' e^{i\phi}$ and width W_s.

- For $W_s \ll \xi$ the middle superconductor hardly affects the gap closing at $\theta = \pm\pi/2$. The coherence length $\xi = \frac{hv_F}{\Delta'}$.
- For $W_s \gg \xi$ the junction breaks into two junctions, with a gap closing at $\phi \pm \theta = \pi$.
- We need a spin dependent v_F.

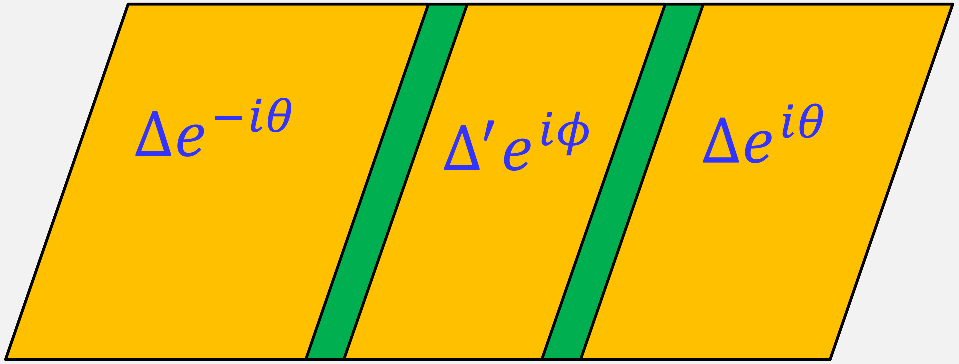

The gap closes at $$\cos\theta + \tanh\frac{W_S}{\xi}\cos\phi = 0$$

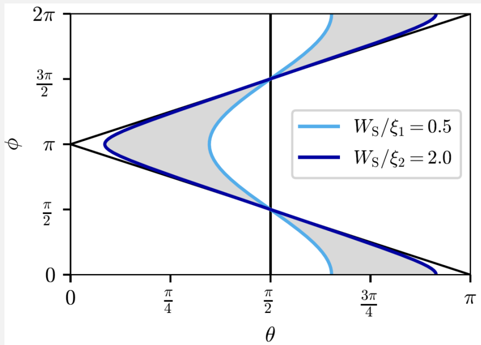

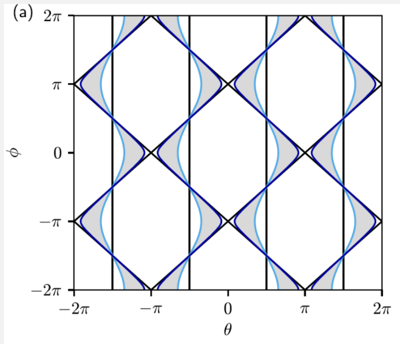

Width of the normal part may shrink ⇒

gap may become close to Δ

$$\cos\theta \quad + \quad \tanh\frac{W_S}{\xi}\cos\phi \quad = \quad 0$$

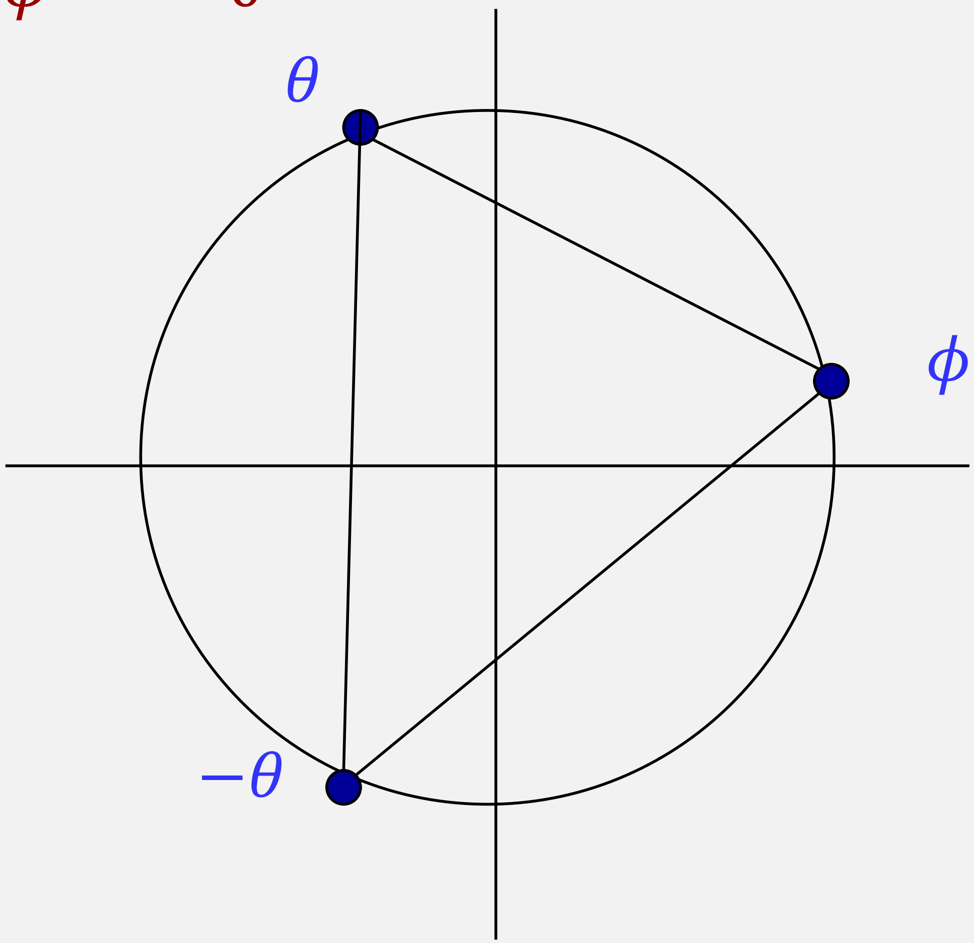

The origin must be within the triangle for topological superconductivity

Different Fermi velocities for the two branches

- Band structure
  HgTe
  TMDs (Ising spin-orbit coupling welcome)
  $MX_2 \quad (M = W, Mo \qquad X = S, Se, Te)$

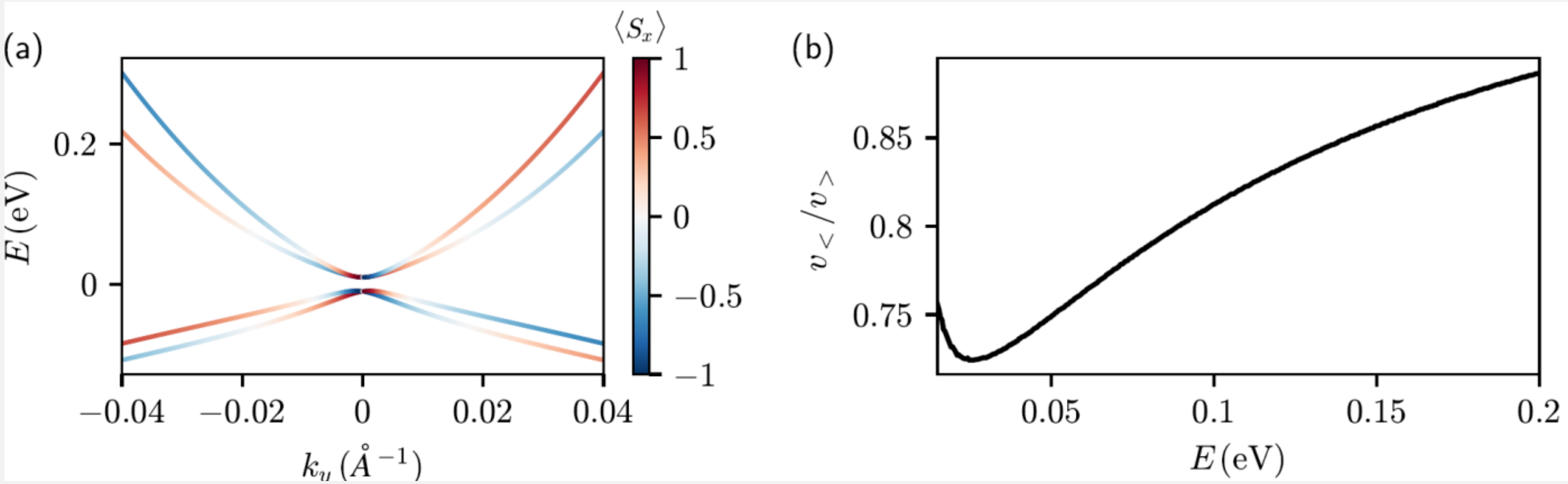

- Proximity to a second sub-band in a hetero-structure
- Periodic potential in the x-direction (Lesser et al.).

Unequal Fermi velocities –
presumption of innocence or presumption of guilt?

The Rashba bias

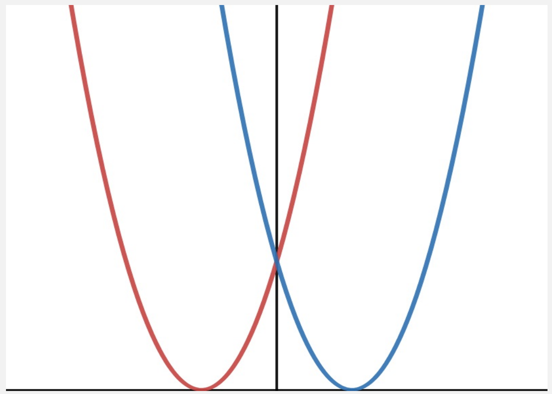

Exact for a 1D ring with nearest neighbor hopping only

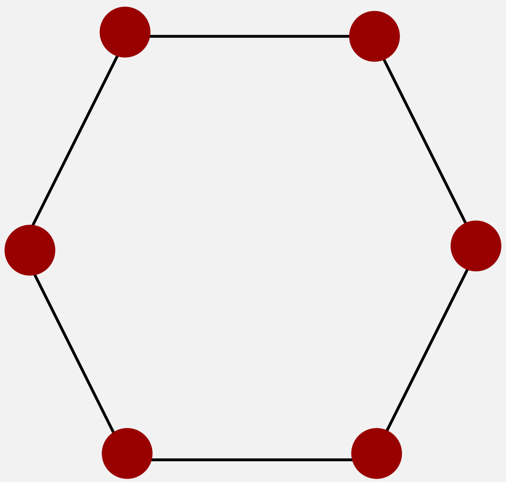

SOC acts like spin-dependent flux (Meir et al., 1989)

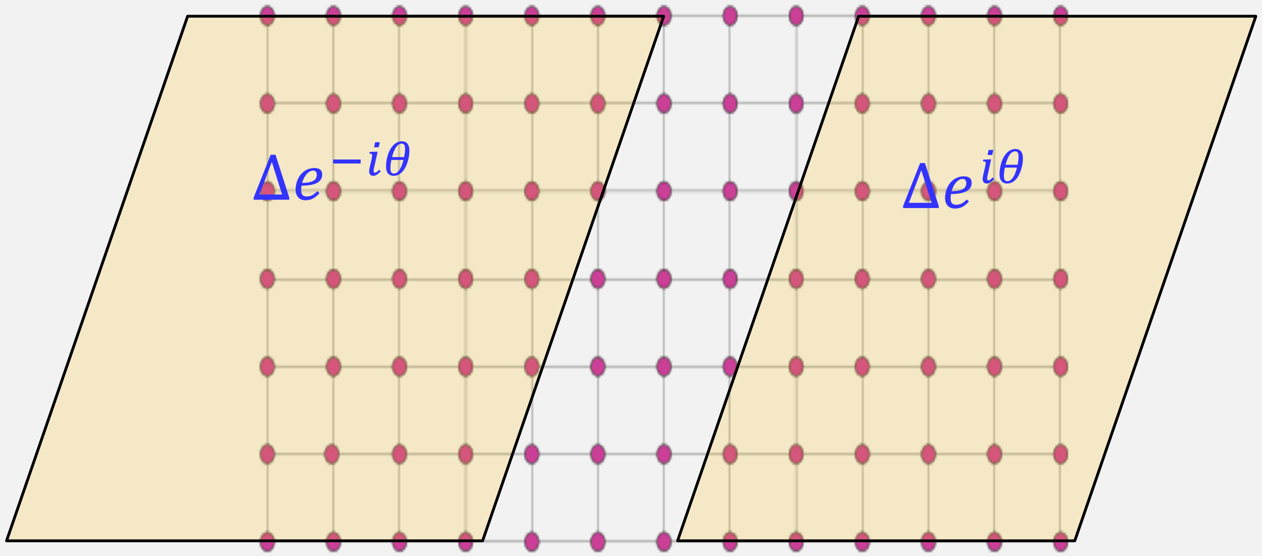

In 2D, nearest neighbor only:

$$H(k) = -\sum_i t_i \cos(k \cdot a_i) - \sum_{i,\alpha} \lambda_{i,\alpha} \sigma_\alpha \sin k \cdot a_i$$

$k_x = 0$ the problem becomes 1D, with longer range hopping

Hetero-structures

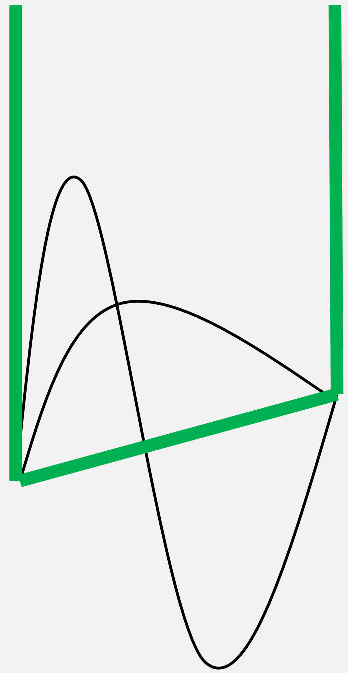

$$H = \frac{p^2}{2m} + V(z) + \alpha(z) k \times \sigma \cdot z$$

$$H = \begin{pmatrix} \frac{k_y^2}{2m} & 0 \\ 0 & \frac{k_y^2}{2m} + \Delta E \end{pmatrix} + \begin{pmatrix} \alpha_{11} & \alpha_{12} \\ \alpha_{12} & \alpha_{22} \end{pmatrix} \mathrm{k_y} \sigma_x$$

$$\alpha_{ij} = \int dz \chi_i(z) \alpha(z) \chi_j(z)$$

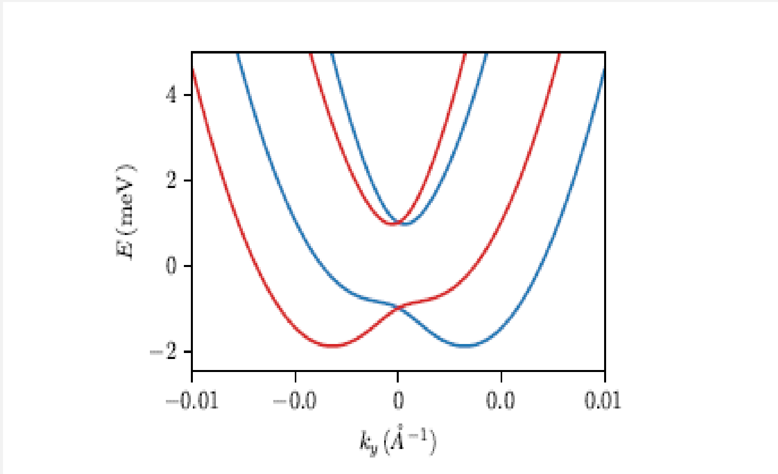

Periodicity in the x-direction (Lesser et al.)

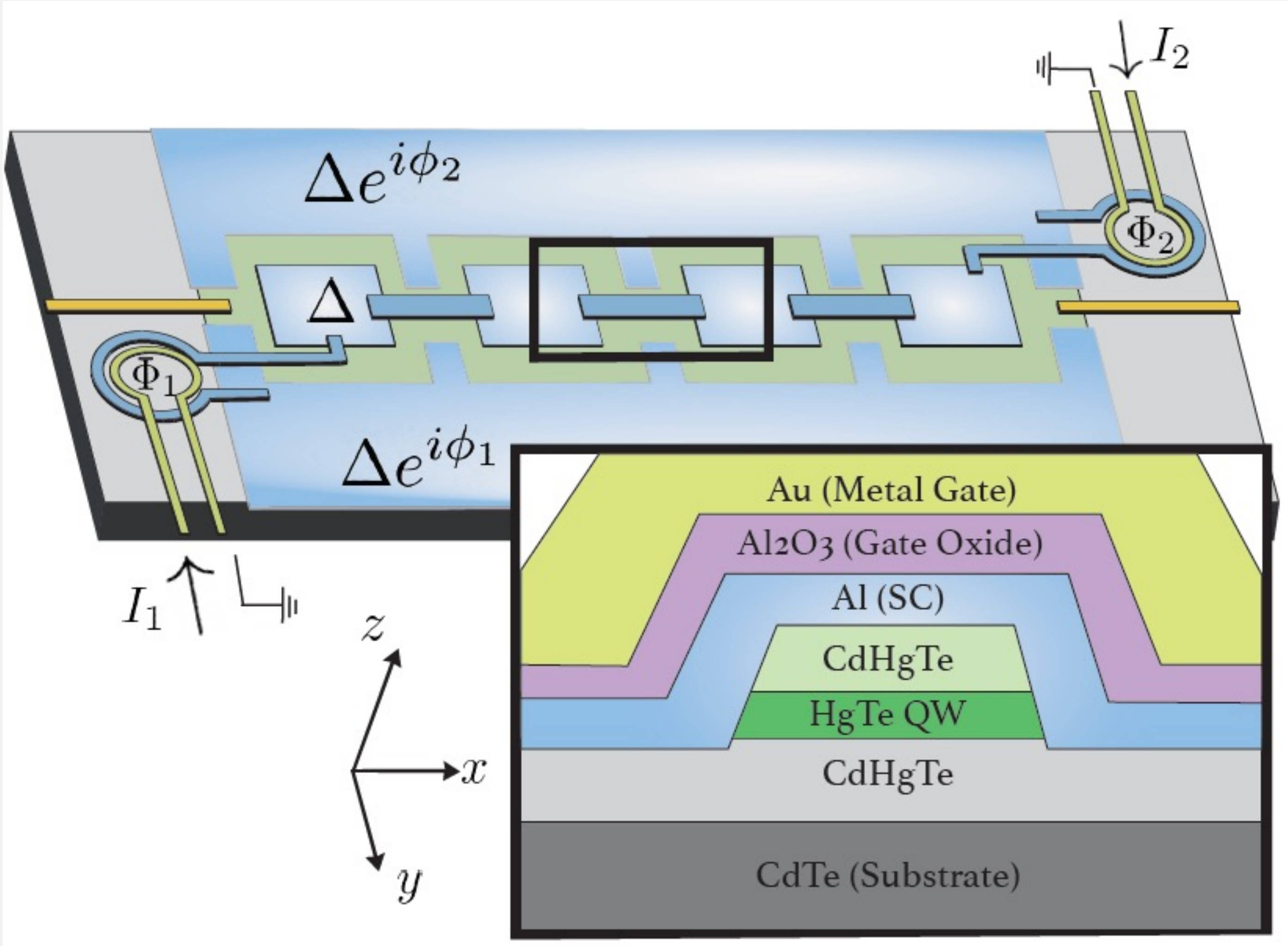

The effect of disorder on the localization of the zero modes

With Arbel Haim (Cal-Tech)

Numerically -

For weak disorder, Majoranas get (significantly) better localized.

In contrast to 1D p-wave superconductors.

Why –

1. Identify the culprit – large k gap

2. The effect of disorder on that gap – combination of selection rules and pairing phases.

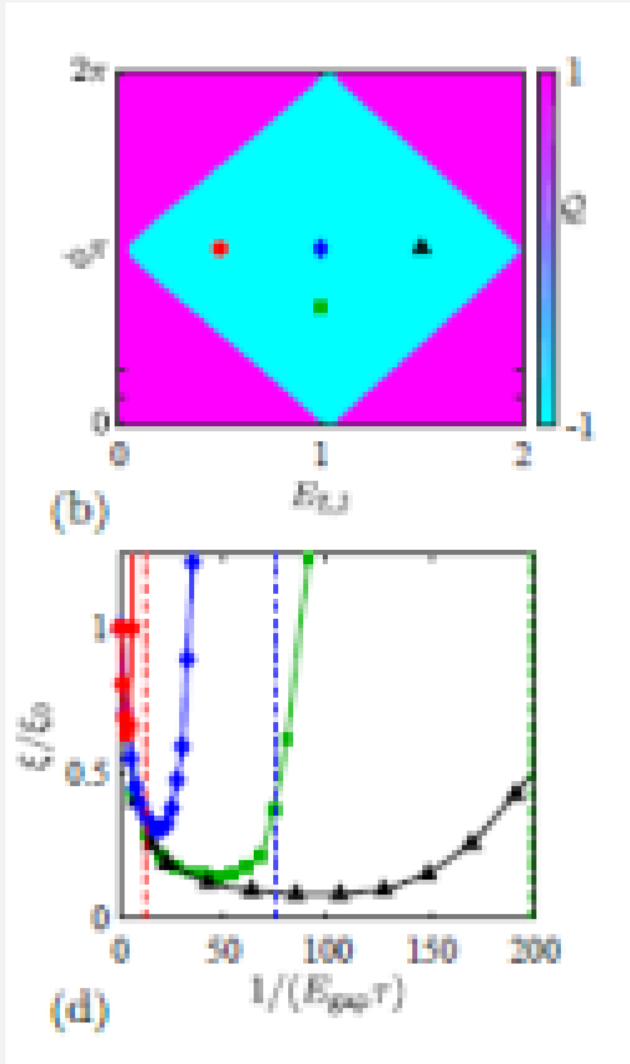

Spectrum of excitations in the topological phase

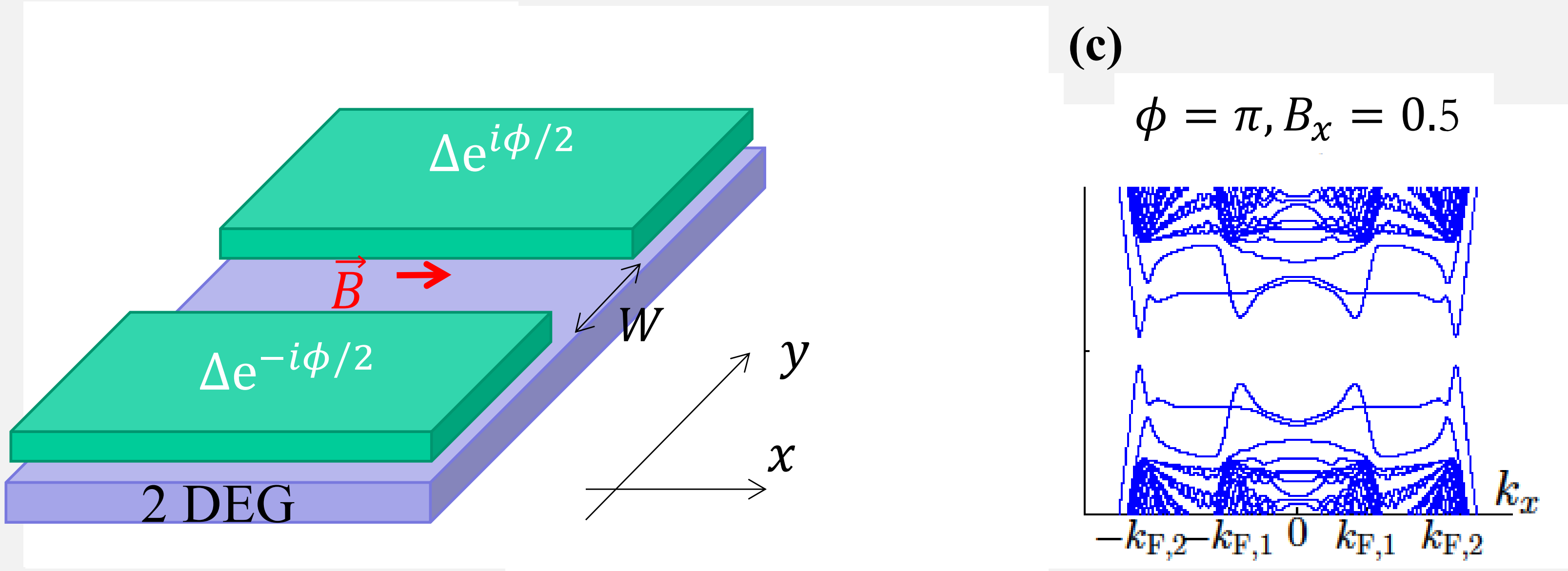

Smallest gap at the two Fermi momenta

Think about the spectrum as coming from pairing of several modes

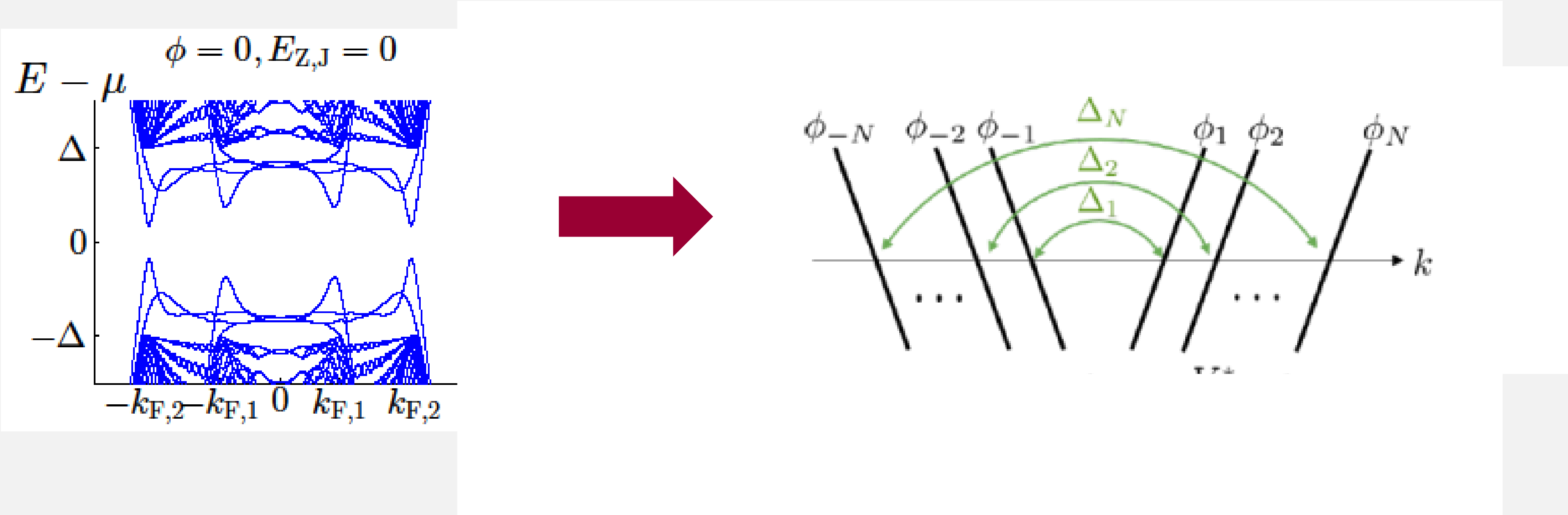

Effect of disorder - perturbative calculation:

Localization length - $\frac{hv_F}{\Delta_{eff}}$

$$\Delta_{eff,m} \approx \Delta_m + \sum_{n \neq m} \frac{1}{\tau_{mn}} e^{i \arg(\Delta_n) + i\alpha_{mn}} \qquad \frac{1}{\tau_{mn}} = \frac{V_{mn}^2}{|v|}$$

$$\Delta_{eff,m} \approx \Delta_m + \sum_{n \neq m} \left(\frac{1}{\tau}\right)_{mn} e^{i \arg(\Delta_n)}$$

- To be affected by a channel, need to be able to scatter into it
- Once scattered into it, the phase of its pairing potential matters.

Particular cases:

- Disorder scattering into the pairing partner – necessarily reduces Δ_{eff} (phase difference of π).

$$\Delta_m c_m^+ c_{-m}^+ \quad \Rightarrow \quad \Delta_m = -\Delta_{-m}$$

- Delocalizes Majorana modes in p-wave superconductors.

- Different situation for s-wave superconductors
  - Selection rule – disorder does not flip spin, so no scattering to pairing partner.
  - No phase difference of pairing potentials.

  - Disorder enhances localization

In our case, large k behaves like s-wave, small k behaves like p-wave

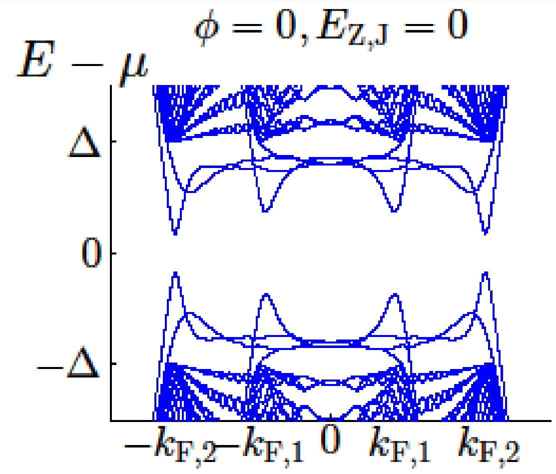

The small k determines topology, the large k determines localization.

Magnetic impurities couple large-k pairing partners, and delocalize the Majorana modes

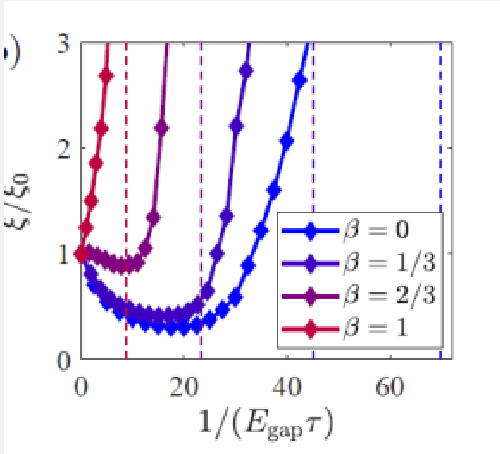

Summary:

Difficulties:

- Uneasy coexistence of superconductivity and magnetic field
- Uneasy coexistence of gating and superconductivity
- Disorder

Solutions:

- Replace the magnetic field by tuning of phases
- Dependence on chemical potential is weak
- Effects of disorder may be weakened